IET Electric Power Applications

*Research Article*

IET Journals
The Institution of Engineering and Technology

# Comparison of stator winding connections in multiphase drives under healthy operation and with one open converter leg

ISSN 1751-8660
Received on 3rd June 2019
Revised 14th October 2019
Accepted on 5th December 2019
doi: 10.1049/iet-epa.2019.0467
www.ietdl.org

*Alejandro G. Yepes[1] ✉, Jesús Doval-Gandoy[1], Fernando Baneira[1], Hamid A. Toliyat[2]*

[1]*Applied Power Electronics Technology Research Group, University of Vigo, Vigo 36310, Spain*
[2]*Department of Electrical and Computer Engineering, Texas A&M University, College Station, TX 77843, USA*
✉ *E-mail: agyepes@uvigo.es*

**Abstract:** Multiphase machines with symmetrical windings offer various stator winding configurations (SWCs). It is known that, for a given five-phase machine, the pentagon SWC implies, compared with star, smaller voltage rating and greater current rating of the converter. For healthy conditions, the stator copper loss (SCL) and maximum achievable torque (MAT) are almost identical for both SWCs, provided such converter-rating adjustments and negligible circulating currents. Regarding the operation of five-phase machines under open converter leg (especially common fault), the pentagon SWC attains lower SCL (for given torque) and larger MAT than star. However, it is unknown if these characteristics hold (and to which extent) for other phase numbers and SWCs. This study compares for multiple phase numbers the SWCs in terms of converter rating, MAT and SCL, under healthy operation and with an open converter leg. Most importantly, it is shown that, for phase numbers higher than five (the case previously studied), the improvement in performance (especially postfault MAT) by resorting to SWCs other than star can be much larger than for five phases, and it is thus of considerable interest. The most convenient alternatives (often different from the five-phase case) are established. Experimental results with two multiphase drives are included.

## 1 Introduction

Multiphase drives offer several important advantages in comparison with three-phase ones, such as reduced current rating and enhanced fault tolerance [1–4]. In fact, fault tolerance in multiphase drives is currently a very active field of research [1–18]. Although various types of faults can occur in electric drives, most of them arise in the power electronics [4, 13]. In this manner, the case of an open leg in the converter is of particular interest [9–11]. Moreover, this fault type also represents the cases when a line is opened by means of an additional protection device (e.g. a switch or fuse) placed between machine and converter [6, 15, 18].

Multiple ac/dc-converter topologies can be employed for fault-tolerant $n$-phase drives, including conventional $n$-leg converters (with two or more levels, and one or several dc links) [1–4], those with the stator neutral connected to the dc-link midpoint or to an extra leg [18–21], and $2n$-leg converters (with common or separate dc links, such as individual H bridges) for open-end windings [1, 2, 13, 16, 20, 21]. For a given machine, the required dc-link voltage and per-leg current rating are similar for all these converter topologies except for those based on open-end windings, for which the dc-link voltage is halved [2, 21]. Furthermore, open-end windings offer higher reliability against stator short-circuit faults and better open-phase performance, due to zero-sequence stator current [16]. However, it comes at the expense of needing access to all winding ends, of the increased number of devices per phase, and hence, also of greater probability of a phase being affected by a switch fault. Converters with neutral connection permit to enhance the postfault capabilities by injecting zero-sequence current, as well, but accessible machine neutral point is required [22] and larger current distortion may arise [20]. In fact, converters with $n$ legs and no neutral connection are undeniably very common in fault-tolerant drives [1–12, 14, 15, 17], and are the ones contemplated hereafter (with either single or separate dc links).

Regarding the spatial angles between stator phases, the usual approaches are to set a $\gamma = 2\pi/n$ displacement between consecutive ones (i.e. a symmetrical winding arrangement – SWA), to set $n/3$ three-phase stars with $\pi/n$ separation between them (i.e. an asymmetrical winding arrangement – AWA), or to set various stars that overlap in space [6]. It is possible to reconfigure a stator with SWA and even $n$, by swapping the polarity of opposite phases, so that it becomes equivalent to the last type (overlapping windings), as done in [23] for $n = 6$. This makes it possible to use just $n/2$ converter legs (with twice the current rating and less tolerance to converter faults), and/or also to improve the dc-link utilisation [23]. Another way to allow for smaller dc-link voltage is to set several stars with independent neutrals [21]. However, among these options, in general, SWA without polarity swapping and with single neutral exhibits the best capabilities (maximum achievable torque – MAT and stator copper loss – SCL) for an open converter leg [6, 14]. Thus, it is the preferred option if postfault performance is a priority, and is the one considered henceforth when referring to star stator winding configuration (SWC).

Although star is by far the most common SWC [24], other possibilities exist [8–12, 24]. An $n$-phase machine with SWA permits up to $\lceil n/2 \rceil$ non-redundant SWCs [8, 12, 24]. For instance, for $n = 3$ star or delta can be used, and for $n = 5$ there are star, pentagon and pentacle SWCs [8–12, 24].

For $n = 5$ with SWA and given machine ratings, the pentagon SWC, when compared with star, permits to reduce the converter voltage rating, at the cost of increased converter current rating [9]. This statement holds for healthy or fault operation, although these differences vary to some degree quantitatively [9]. In the absence of faults, the MAT (equivalent then to rated torque) and the SCL may be slightly (with proper machine design) smaller and larger, respectively, for pentagon SWC, due to undesired circulating zero-sequence current [9, 10]. With an open converter leg, the pentagon SWC offers lower SCL (for given torque) and larger MAT [9–11], which is the maximum torque that can be achieved without exceeding the machine rated current. However, although these facts were shown for $n = 5$ [9–11], it is unclear if they also hold for greater $n$ and other SWCs, and if so, to which extent. Thus, it is important to analyse the MAT, SCL and converter rating for various SWCs when $n$ is higher than five.

This paper compares the differences between SWCs for $n$-phase drives, under healthy conditions and with an open converter leg. For the first time, the MAT (or equivalently, derating factor – DF), SCL and converter rating are assessed for each SWC and $n$ up to 15 (higher $n$ is extremely rare). Most importantly, it is shown that the performance (especially postfault MAT) with $n$ other than five

can be improved, by exploiting the SWCs, to a much greater extent than for the previously known case of $n = 5$. For some $n$, the variation of the converter rating with the SWCs also differs substantially from the known behaviour with $n = 5$. The most convenient combinations of $n$ and SWCs are determined. Experimental results with two multiphase drives are provided to support the theoretical analysis. In the preliminary version [25] the converter rating was not taken into account, in spite of its relevance for fault-tolerant drives [9, 26], and it did not contain experimental results.

The paper is organised as follows. Section 2 reviews the vector space decomposition, the relation between torque and stator current, the MAT and DF concepts, and the SWCs. Section 3 describes the optimum currents for an open converter leg and any SWC. The performance in terms of MAT, SCL and converter rating is compared in Sections 4–6, respectively. Experimental results are presented in Section 7. Finally, Section 8 concludes the work.

## 2 Background

### 2.1 Vector space decomposition

Regardless of the SWC, an $n$-phase machine with SWA can be modelled in $m = \lfloor n/2 \rfloor + 1$ orthogonal subspaces by using the vector space decomposition, e.g. the general form given in [14]. Namely, in $P = \lceil n/2 \rceil - 1$ planes and one or two (for odd or even $n$, respectively) zero-sequence axes [14]. AWAs are deemed to be out of the scope of this paper, for any SWC. A stator electrical variable $u$ (e.g. voltage $v$ or current $i$) given in stator per-phase values can be transformed as [14, 24]

$$\begin{bmatrix} u_{\alpha_1} & u_{\beta_1} & u_{\alpha_2} & u_{\beta_2} & \dots & u_{\alpha_P} & u_{\beta_P} & u_{0^+} & u_{0^-} \end{bmatrix}^{\mathrm{T}} = \boldsymbol{H} \begin{bmatrix} u_a & u_b & \dots & u_n \end{bmatrix}^{\mathrm{T}} \tag{1}$$

with $\boldsymbol{H}$ being the magnitude-invariant transformation matrix

$$\boldsymbol{H} = \frac{2}{n} \begin{bmatrix} 1 & \cos(\gamma) & \cos(2\gamma) & \dots & \cos(n'\gamma) \\ 0 & \sin(\gamma) & \sin(2\gamma) & \dots & \sin(n'\gamma) \\ 1 & \cos(2\gamma) & \cos(4\gamma) & \dots & \cos(2n'\gamma) \\ 0 & \sin(2\gamma) & \sin(4\gamma) & \dots & \sin(2n'\gamma) \\ \vdots & \vdots & \vdots & \ddots & \vdots \\ 1 & \cos(n'\gamma) & \cos(2n'\gamma) & \dots & \cos\left[(n')^2\gamma\right] \\ 0 & \sin(n'\gamma) & \sin(2n'\gamma) & \dots & \sin\left[(n')^2\gamma\right] \\ 1/2 & 1/2 & 1/2 & \dots & 1/2 \\ 1/2 & -1/2 & 1/2 & \dots & -1/2 \end{bmatrix} \tag{2}$$

where $\gamma = 2\pi/n$ and $n' = n - 1$. The phase order ($u_a$, $u_b$, etc.) in the vector in the right-hand side of (1) is assumed to match the spatial sequence of phases in the stator [14]. In accordance with (1) and (2), the penultimate and the last rows of $\boldsymbol{H}$ correspond with the $u_{0^+}$ and $u_{0^-}$ zero-sequence components, respectively. The latter only exists if $n$ is even; otherwise, it is omitted. If the space harmonics are disregarded, the resulting $u_{\alpha_1}$ and $u_{\beta_1}$ variables are related to flux and torque, whereas the rest ($u_{\alpha_2}$, $u_{\beta_2}$, etc.), only to losses [1]. The existing space harmonics in a particular machine may give rise to additional losses, saturation, torque ripple and requirement of dc-link voltage, and they can be taken into account in practice to, e.g. improve the torque density to a certain extent [7, 19, 27]. Moreover, their effect on the airgap flux distribution may change with the SWC [10]. Nevertheless, they are neglected in this paper, as often done in publications about multiphase drives under fault [4–6, 14], to allow for a more general study, regardless of, e.g. specific distributions of the stator coils. Such effects would normally be, in any case, of much smaller importance than those of the fundamental component, which are addressed here.

### 2.2 Calculation of $i_{\alpha_1}$ and $i_{\beta_1}$ for torque generation

It is convenient to define a frame with orthogonal axes $d$ and $q$ rotating in the $\alpha_1 - \beta_1$ plane, with the $d$-axis being aligned with the rotor flux (i.e. field-oriented) [28]. The corresponding dc current references $i_d$ and $i_q$ in this synchronous frame can be calculated so as to yield a certain torque [28]

$$T = \frac{n}{2} N_p (\psi_d i_q - \psi_q i_d) \tag{3}$$

where $N_p$ is the number of pole pairs, and $\psi_d$ and $\psi_q$ designate the stator flux linkage along with the $d$- and $q$-axes, respectively. Throughout the paper, for simplicity, no difference is made in the notation to distinguish the reference signals from the actual ones. In a synchronous machine, the stator flux linkages in (3) are [28]

$$\psi_d = L_d i_d + \psi_r; \quad \psi_q = L_q i_q \tag{4}$$

where $\psi_{\mathrm{r}}$ is the flux produced by the rotor (e.g. by permanent magnets), if any (e.g. $\psi_{\mathrm{r}} = 0$ in synchronous reluctance machines), and $L_d$ and $L_q$ denote the stator self-inductance in the $d$- and $q$-axes, respectively. In an induction machine, the flux linkages are instead [28]

$$\psi_d = \frac{L_{\mathrm{m}}}{L_{\mathrm{r}}} \underbrace{L_{\mathrm{m}} i_d}_{\psi_{\mathrm{r}}} + L'_{\mathrm{s}} i_d; \quad \psi_q = L'_{\mathrm{s}} i_q \tag{5}$$

where $L_{\mathrm{m}}$ stands for magnetising inductance, $L_{\mathrm{r}}$ for rotor self-inductance, and $L'_{\mathrm{s}}$ for stator transient inductance. The $\psi_{\mathrm{r}}$ expression shown in (5) may not hold during transients, but it does in steady-state [28]. Equations (3)–(5) are valid for either healthy or fault situations [5, 6, 14].

For a certain machine and $T$ value, the substitution of (4) or (5) into (3) gives one equation and two unknowns: $i_d$ and $i_q$. Another equation, involving $i_d$, is typically added, e.g. to fix $i_d = 0$ (non-salient synchronous machines in the base-speed region), to set the rated flux with $i_d$ (induction machines in the base-speed region), to ensure maximum-torque-per-ampere operation (salient synchronous machines), or to additionally decrease $\psi_d$ (field-weakening region) [28]. From the $i_d$ and $i_q$ dc references, the $i_{\alpha_1}$ and $i_{\beta_1}$ ac ones are obtained by a rotational transform [28].

### 2.3 Maximum achievable torque and DF

Let us assume that the converter voltage and current ratings are adequately adjusted (addressed later) so that they are not surpassed after a leg is open. Then, the maximum torque that can be provided while complying with the machine current rating $i^{\mathrm{rc}}$ (i.e. the MAT) is reduced in respect to a healthy situation. Note that rc stands for rated conditions. This MAT decrease is often referred to as derating, and its quantification is important to assess the postfault performance [5, 6, 14].

The DF is defined as the maximum attainable (without exceeding $i^{\mathrm{rc}}$ in any phase) value of the current reference $\alpha_1 - \beta_1$ modulus

$$\left|i_{\alpha_1\beta_1}\right| = \sqrt{i_{\alpha_1}^2 + i_{\beta_1}^2} = \sqrt{i_d^2 + i_q^2} \tag{6}$$

with the latter being normalised with respect to rated healthy conditions (henceforth, simply 'normalised'), i.e. divided by $\left|i^{\mathrm{rc}}_{\alpha_1\beta_1}\right| = i^{\mathrm{rc}}$ [6]. The DF is strongly related to the MAT [5, 6], as can be inferred from (6) and Section 2.2. For a certain machine, a larger DF in general also means a higher MAT, and vice versa [6]. On the other hand, unlike the MAT, for given $n$, SWC and fault, the DF is independent of how the $\left|i_{\alpha_1\beta_1}\right|$ quantity is distributed between $i_d$ and $i_q$ ($i_d/i_q$ ratio). That is, the DF does not depend on the operation region (base-speed or field-weakening), machine type (induction, permanent-magnet, etc.), rated power or machine

parameters [6]. The reasons for this independence may be better understood once the calculation of the other current references and the DF is explained in detail, later on. Consequently, the DF can be used to indirectly study the MAT performance in a general manner [6]. Numerical examples of the relation between the DF and MAT will also be given in the experimental results.

### 2.4 Types of SWCs

In an $n$-phase machine with SWA it is possible to set $\lceil n/2 \rceil = P + 1$ different SWCs [8, 12, 24]. An SWC is obtained by connecting in series every pair of phases such that the spatial step between them (between, e.g. their north-pole axes) spans $\lambda$ consecutive phases (north-pole axes). Note that here the term 'series' is used to describe the SWC by ignoring, for simplicity, the connection that is eventually done between the stator terminals and the converter legs. Thus, each $\lambda$ value, from zero (star) to $P = \lceil n/2 \rceil - 1$, results in a different SWC.

For instance, the SWCs in a six-phase machine are depicted in Fig. 1, for $\lambda = 0$, 1 and 2. The star SWC corresponds to $\lambda = 0$ (see Fig. 1*a*). When $\lambda = 1$, each phase is connected in series with the one that follows in the stator physical disposition (see Fig. 1*b*). Finally, $\lambda = 2$ means that the series connections are made in steps of two phases with respect to the spatial order of the windings (see Fig. 1*c*), i.e. a with $c$, $b$ with $d$, etc. A line current $i_{\phi_1\phi_2}$ (supplied by the converter) equals $i_{\phi_1} - i_{\phi_2}$, with $\phi_1$ and $\phi_2$ being two phases connected in series.

When $\lambda > 1$ and $n/\lambda \notin \mathbb{Z}$, the stator phases form a single electrical loop, as for $\lambda = 1$. This happens, e.g. for $n = 5$ and $\lambda = 2$ [8, 12]. On the contrary, when $n/\lambda \in \mathbb{Z}$, the stator phases form $\lambda$ loops. For instance, for $n = 6$ and $\lambda = 2$, two delta circuits are obtained, as depicted in Fig. 1*c*.

As aforesaid, for $\lambda = 0$ one neutral point is assumed, since, for open phase, it yields higher MAT and smaller SCL than several [5, 6]. Hence, if in the following analysis a certain SWC is shown to give a superior postfault performance in terms of MAT and SCL compared with a single star, it implies that the former SWC is also preferable in this regard over an SWC based on various separate stars. Analogous reasoning could be applied for other $\lambda = 0$ approaches that also present worse postfault performance, such as swapping the polarity of some phases if $n$ is even [6, 23] or using AWA [6, 14].

## 3 Postfault current references for different SWCs

A strategy for the generation of current references for the open phase and $\lambda = 0$ was presented in [14]. Unlike other techniques, such a method provides minimum SCL for any given torque and is also able to attain the postfault MAT. It can be adopted as a benchmark for comparing the postfaul potential of different SWCs. In this section, prior to the comparative analysis, the current-reference strategy from [14] is extended to any $\lambda$. This extension is relatively straightforward and is not claimed to be a relevant contribution.

For given $\alpha_1 - \beta_1$ current (flux, torque and core loss) references computed according to Section 2.2, the other current references can be written as a function of these ones [5, 6, 14]

$$\begin{bmatrix} i_{\alpha_1} & i_{\beta_1} & i_{\alpha_2} & i_{\beta_2} & \cdots & i_{\alpha_P} & i_{\beta_P} & i_{0^+} & i_{0^-} \end{bmatrix}^{\mathrm{T}} = \boldsymbol{H}_k \begin{bmatrix} i_{\alpha_1} & i_{\beta_1} \end{bmatrix}^{\mathrm{T}} \tag{7}$$

where $\boldsymbol{H}_k$ is the coefficient matrix

$$\boldsymbol{H}_k = \begin{bmatrix} 1 & 0 & k_{\alpha_2,\alpha} & k_{\beta_2,\alpha} & \cdots & k_{\alpha_P,\alpha} & k_{\beta_P,\alpha} & k_{0^+,\alpha} & k_{0^-,\alpha} \\ 0 & 1 & k_{\alpha_2,\beta} & k_{\beta_2,\beta} & \cdots & k_{\alpha_P,\beta} & k_{\beta_P,\beta} & k_{0^+,\beta} & k_{0^-,\beta} \end{bmatrix}^{\mathrm{T}} \tag{8}$$

.

Analogously to [14], the optimum $\boldsymbol{H}_k$ for each $|i_{\alpha_1\beta_1}|$ value results by minimising the normalised SCL (cost function)

$$J = \frac{\boldsymbol{I}^{\mathrm{T}}\boldsymbol{I}}{(i_d^{\mathrm{rc}})^2 + (i_q^{\mathrm{rc}})^2} = \frac{\boldsymbol{I}^{\mathrm{T}}\boldsymbol{I}}{(i^{\mathrm{rc}})^2} \tag{9}$$

with $\boldsymbol{I}$ being the current vector in the left-hand side of (7), while satisfying for any $\alpha_1 - \beta_1$ phase angle the restrictions

$$i_{\mathrm{fl}} = 0 \tag{10}$$

$$\max\{|i_\phi|\}/i^{\mathrm{rc}} \leq 1, \quad \phi = a, b, \ldots, n \tag{11}$$

where fl stands for faulted line, and also obeying one (if $\lambda = 0$ or $n/\lambda \notin \mathbb{Z}$) or $\lambda$ (if $n/\lambda \in \mathbb{Z}$) additional constraint equations

$$\sum_{\phi \in \Phi} i_\phi = 0 \tag{12}$$

where $\Phi$ contains all phases ($\lambda = 0$) or those in a loop ($\lambda \neq 0$).

When $\lambda = 0$, $i_{\mathrm{fl}}$ in (10) simply represents a stator phase current [14]. Otherwise, if $\lambda \neq 0$, then $i_{\mathrm{fl}} = i_{\phi_1\phi_2} = i_{\phi_1} - i_{\phi_2}$, with $\phi_1$ and $\phi_2$ being the corresponding pair of phases. In some previous postfault strategies [9], (11) is replaced by the less conservative requirement of not surpassing the prefault total SCL, but this may cause hot spots and damage the machine insulation [4]. Nevertheless, in qualitative terms, the conclusions of the comparison between SWCs are not expected to change considerably depending on this choice.

Note that for $\lambda = 0$ (12) reflects the Kirchoff current law applied to the stator windings, whereas for $\lambda \neq 0$ (12) follows from the Kirchoff voltage law. For example, for $n = 6$ and $\lambda = 2$, (12) gives two equations, involving three phases each, which correspond to the two delta loops formed by the stator windings (see Fig. 1*c*). A consequence of (12) is that $i_{0^+} = 0$ and $k_{0^+,\alpha} = k_{0^+,\beta} = 0$ are always satisfied in (7) and (8).

In agreement with (9)–(12), for a given normalised $|i_{\alpha_1\beta_1}|$ value, the resulting $\boldsymbol{H}_k$ and hence the associated normalised SCL and required converter rating are independent of the $i_d/i_q$ ratio, machine parameters (e.g. inductances and resistances), machine type, rated power and operation region (base-speed or field-weakening).

For the analysis in the following sections, the problem (9)–(12) is solved by running the *fmincon* function in Matlab with the

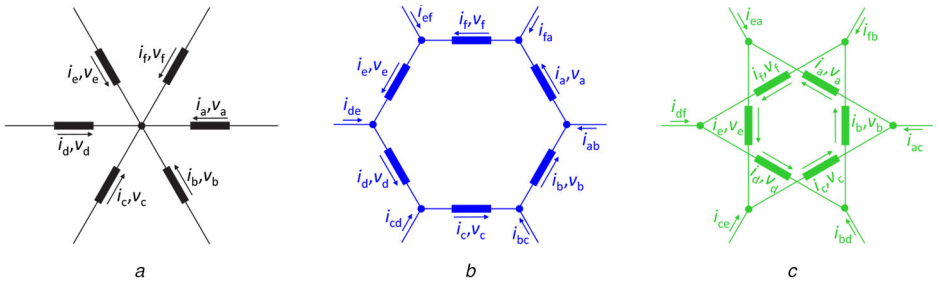


**Fig. 1** *SWCs in a six-phase machine*
***(a)***, $\lambda = 0$, ***(b)***, $\lambda = 1$, ***(c)***, $\lambda = 2$

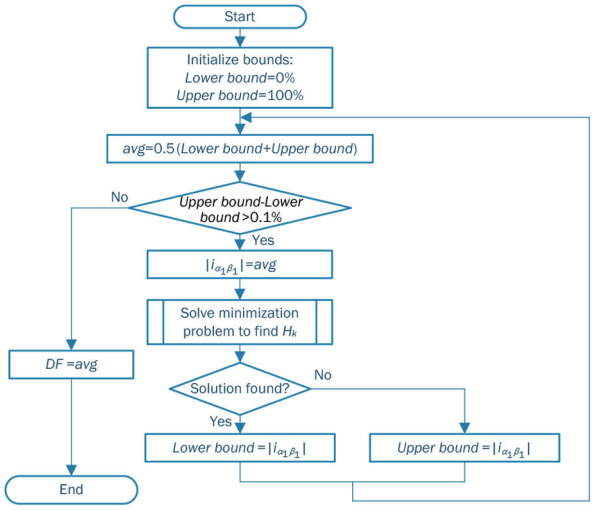


**Fig. 2** *Algorithm to find the DF for a given n and SWC*

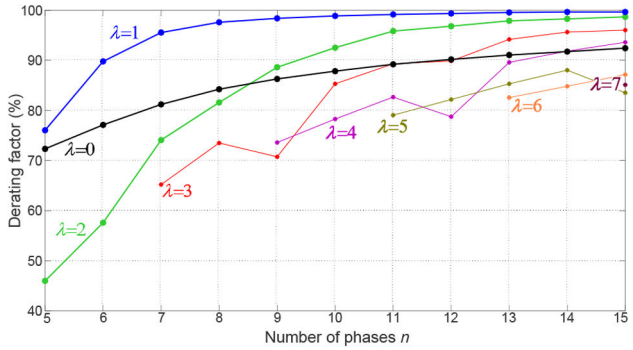


**Fig. 3** *DF as a function of n and the SWC*

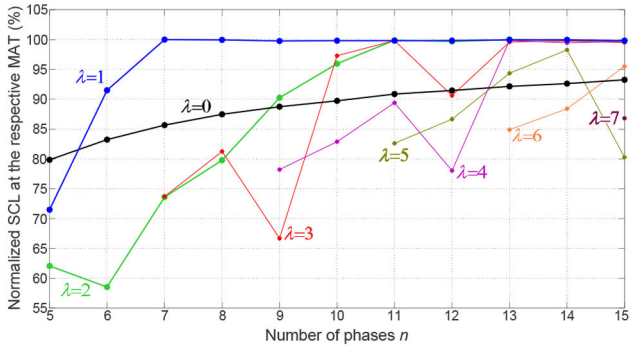


**Fig. 4** *Normalised SCL, as a function of n and the SWC, at the respective MAT*

*active-set* solver [14]. *MultiStart* is used to generate 200 different starting points, so that the global minimum is found.

Since $\boldsymbol{H}_k$ varies with required torque, its coefficients can be stored in look-up tables when implemented in a drive [14].

In the subsequent theoretical study, actual currents are assumed to track the references perfectly, i.e. the non-ideal effects of the closed-loop current control are disregarded.

## 4 Comparison of maximum achievable torque

In a healthy drive, with space harmonics disregarded (see Section 2.1), the MAT equals the rated torque (DF = 100%) for any SWC. In practice, the DF may be slightly lowered due to currents circulating in the stator loops for $\lambda \neq 0$, depending on the particular machine and its space harmonics [9]. Regarding postfault operation, the algorithm in Fig. 2 is used to find the DF for given $n$ and SWC. It is based on the fact that, as $|i_{\alpha_1\beta_1}|$ rises, it becomes increasingly difficult to satisfy (11), until it is not possible anymore. Accordingly, in Fig. 2 the gap between a *lower bound* and an *upper bound* of $|i_{\alpha_1\beta_1}|$ is iteratively reduced, by changing one of them depending on whether a solution $\boldsymbol{H}_k$ for (9)–(12) is found or not for a normalised $|i_{\alpha_1\beta_1}|$ equal to the average (*avg*) of such bounds. The difference between the $|i_{\alpha_1\beta_1}|$ bounds is decreased in every iteration until it is below 0.1%, and then the *avg* value is assigned to the DF.

As aforementioned, for given normalised $|i_{\alpha_1\beta_1}|$ the solution of the minimisation problem (9)–(12) does not depend on the machine type, parameters, rated power, $i_d/i_q$ ratio and operation region. Thus, it can now be more easily understood from Fig. 2 that, as stated in Section 2.3, the DF is independent of these aspects as well [6].

Fig. 3 shows the resulting DF for each $n$ and SWC. It can be observed that the $\lambda = 0$ DF is not the largest one, compared with the other SWCs, for any $n$. With $\lambda \neq 0$, in general for each $n$, the DF decreases with growing $\lambda$. The exceptions to this statement that can be seen in Fig. 3 are due to the additional restrictions in (12) when $n/\lambda \in \mathbb{Z}$ with $\lambda > 1$; note the DF reductions that occur for $n = 9$ and $\lambda = 3$, for $n = 12$ and $\lambda = 3$ or $\lambda = 4$, and for $n = 15$ and $\lambda = 3$ or $\lambda = 5$. More importantly, $\lambda = 1$ always yields the greatest DF of all SWCs. Moreover, the $\lambda = 1$ plot rapidly approaches 100% as $n$ increases moderately. Conversely, the $\lambda = 0$ curve, e.g. barely surpasses 90% for very high $n$. Although for $n > 15$ the DF with $\lambda = 0$ might also be very close to 100%, so large $n$ is hardly considered in the literature [1, 3, 4].

Even though the improvement of DF for $\lambda = 1$ with respect to $\lambda = 0$ is noticeable for $n = 5$ (3.7%) and has been previously recognised as such [9–11], it is clear from Fig. 3 that the advantage is substantially greater for other $n$ values, such as $n = 6$ (12.7%) or $n = 7$ (14.3%). Even for $n = 15$, when the difference becomes shorter again, it is still 7.2%.

It should also be remarked that, from Fig. 3, when $n > 10$ the MAT associated to $\lambda = 2$ is also very close to that of $\lambda = 1$, and much larger than for $\lambda = 0$.

## 5 Comparison of SCL

In healthy conditions, as for the MAT, in terms of SCL, the only difference between SWCs is that the SCL is moderately larger for $\lambda \neq 0$ due to circulating currents, depending on the machine design [9]. The SCL under fault is addressed next.

Fig. 4 compares the normalised SCL obtained [from the minimisation problem (9)–(12)] for the same $n$ values and SWCs as in Fig. 3, evaluated at the respective MAT of each $n$ and SWC pair. It can be seen in Fig. 4 that, when $\lambda = 0$, the SCL at the MAT increases with $n$. Concerning $\lambda = 1$, in most cases, the SCL is roughly 100%, since all phase currents have then magnitudes equal to the rated current. It is not surprising that in many cases, the SCL is greater for $\lambda \neq 0$ than for $\lambda = 0$, given that the MAT (or DF) is, in numerous instances also larger (see Fig. 3). In a similar manner, the lowest SCL peaks in Fig. 4 mostly correspond to the cases such that $\lambda > 1$ and $n/\lambda \in \mathbb{Z}$, where the DF also decreases in Fig. 3 with respect to the general trend of the plots.

Although Fig. 4 as aforesaid, contains some useful information, for a fair SCL comparison among the SWCs, for each $n$, the SCL should be evaluated at the same torque in all SWCs. This is done in Fig. 5, in which the SCLs are calculated at the MAT of the $\lambda = 0$ SWC for the respective $n$. Accordingly, the $\lambda = 0$ curves in Figs. 4 and 5 are identical. No data is shown in Fig. 5 for the combinations of $n$ and $\lambda$ such that the DF (see Fig. 3) is lower than the DF of the $\lambda = 0$ SWC for the same $n$ (e.g. $n = 7$ with $\lambda = 2$). Most importantly, from Fig. 5, $\lambda = 1$ in general yields the smallest SCL. The fact that $\lambda = 1$ produces lower SCL than the conventional $\lambda = 0$ SWC for a given torque was known for $n = 5$ [9–11], but not for higher $n$. This figure shows that the difference between $\lambda = 0$ and $\lambda = 1$ is considerable for $n \neq 5$ as well, and that $\lambda = 1$ is also preferable compared with other SWCs. In any case, similarly to the behaviour regarding DF (see Fig. 3), for $n > 10$ the SCL with $\lambda = 2$ is also very similar to that of $\lambda = 1$, and significantly better than for $\lambda = 0$ (see Fig. 5).

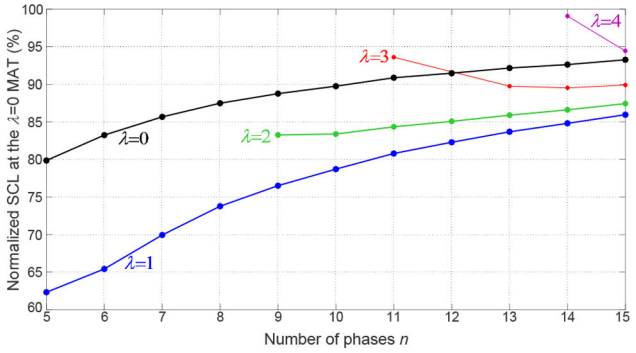


**Fig. 5** *Normalised SCL, as a function of n and the SWC, for torque equal to the $\lambda = 0$ MAT of the respective n*

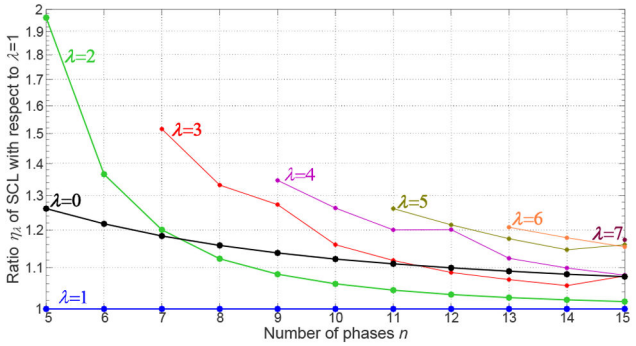


**Fig. 6** *Ratio $\eta_\lambda$ [see (13)], as a function of n and the SWC*

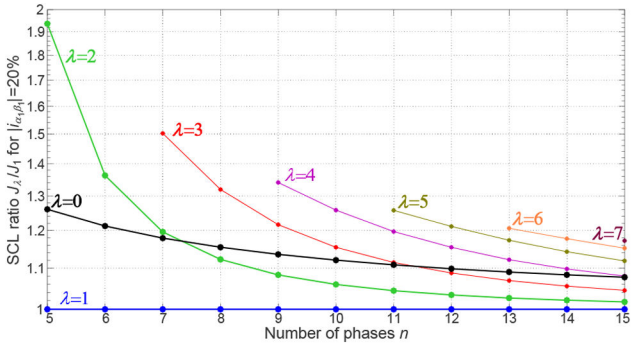


**Fig. 7** *$J_\lambda/J_1$, as a function of n and the SWC, for $|i_{\alpha_1\beta_1}| = 20\%$*

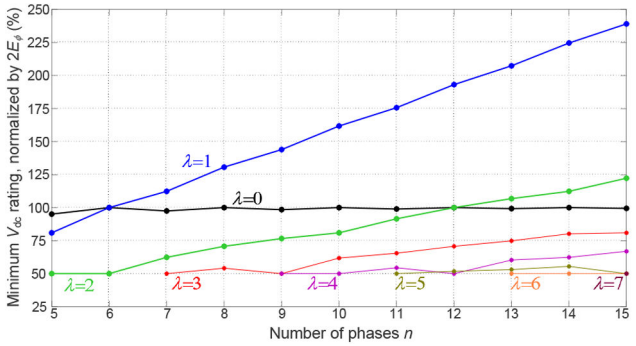


**Fig. 8** *Required dc-link voltage $V_{dc}$, as a function of n and the SWC. Neglecting the stator-impedance voltage drop, these plots are valid for a healthy drive or (roughly) open converter leg*

Although the torque selected for Fig. 5 is representative, it is not clear if the conclusions drawn from it can be applied to other torque values. To perform a more general SCL analysis, the following ratio is defined:

$$\eta_\lambda = \frac{\int_0^{\delta_\lambda i^{rc}} J_\lambda d|i_{\alpha_1\beta_1}|}{\int_0^{\delta_\lambda i^{rc}} J_1 d|i_{\alpha_1\beta_1}|} \tag{13}$$

where $\delta_\lambda$ and $J_\lambda$ are the DF and the SCL, respectively, for the $\lambda$ SWC. In (13), the numerator and the denominator represent the area of the SCL-versus-$|i_{\alpha_1\beta_1}|$ curve for any given $\lambda$ and for $\lambda = 1$, respectively, and both for the same $n$. Note that the integral in the denominator is not evaluated up to the MAT of $\lambda = 1$; on the contrary, the upper limit of both integrals is the MAT of the $\lambda$ variable. On the other hand, $J_1$ is adopted as the reference curve (instead of, e.g. $J_0$) because $\lambda_1$ always gives the largest MAT or DF (see Fig. 3), and thus, it is ensured in this way that the denominator integral in (13) can be computed up to the MAT of $\lambda$ (i.e. up to $\delta_\lambda i^{rc}$).

Fig. 6 shows the $\eta_\lambda$ for various $n$ and SWCs, with a vertical logarithmic scale. The integrals in (13) are computed by the discrete Tustin approximation, with torque steps of 1%. Fig. 6 confirms that $\lambda = 1$ provides the smallest SCL not only for the particular torque values considered in Fig. 5, but for other torque references in general. It is also verified that $\lambda = 2$ can be a good choice from the SCL standpoint when $n > 10$. In addition, it has been checked that the minimum of $J_\lambda - J_1$, for the $n$ and SWCs under consideration and for all possible torque values, is zero (not negative), i.e. $J_\lambda \geq J_1$. Furthermore, it can be seen in Fig. 6 that the difference between SWCs is larger for low $n$, although still notable for high $n$.

In any case, since $J_\lambda$ rises with $|i_{\alpha_1\beta_1}|$, it could be argued that (13) may not be representative of the SCL behaviour for low $|i_{\alpha_1\beta_1}|$. To refute this possibility, the SCL ratio $J_\lambda/J_1$ is shown in Fig. 7 for a relatively small $|i_{\alpha_1\beta_1}|$ value: 20%. The resulting curves in Fig. 7 are very similar to those previously shown in Fig. 6, thus confirming that the conclusions are drawn from Fig. 6 can also be also applied for low $|i_{\alpha_1\beta_1}|$.

## 6 Comparison of converter rating

### 6.1 Comparison of dc-link voltage rating

Assuming that the pulse-width modulation (PWM) injects a suitable non-current-producing voltage, the minimum $V_{dc}$ to avoid overmodulation equals the maximum line-to-line voltage among the converter ac outputs such that there is a possible path for current between them (i.e. they correspond to the same winding loop or star) [21]. For generality, the stator-impedance voltage drop is neglected in comparison with the back-electromotive force (BEMF). This assumption is often made, e.g. when establishing approximately the decrease in maximum speed in fault-tolerant drives [26]. Hence, the necessary $V_{dc}$ can be obtained by calculating the maximum line-to-line voltage (within a loop or a star), based on the BEMFs, for each scenario. Ideally, the phase BEMFs under open converter legs (and hence the $V_{dc}$ needed) are the same as in a healthy situation, as occurs with the $\alpha_1 - \beta_1$ current. Furthermore, the non-current-producing voltage introduced for maximum dc-link utilisation [21] diminishes the effect of the voltage imbalance that occurs after a fault. For a certain machine, the designer could later obtain a more accurate assessment of the required $V_{dc}$, taking into account its parameters, analogously to what is done in other papers for specific machines and faults [9, 17].

Fig. 8 represents the minimum $V_{dc}$ needed depending on $n$ and the SWC. The $V_{dc}$ values are normalised by twice the amplitude of the per-phase BEMF $E_\phi$, i.e. by $2E_\phi$. For $\lambda = 0$ and even $n$, the minimum $V_{dc}$ is $2E_\phi$, since for each phase BEMF there is another with opposite phase angle. For $\lambda = 0$ and odd $n$, the maximum line-to-line voltage is

$$V_{dc}^{rat} = \left|E_\phi - E_\phi e^{j(\pi - (\gamma/2))}\right| = E_\phi \left|1 - e^{j\pi((n-1)/n)}\right| \tag{14}$$

which converges to $2E_\phi$ as $n$ grows, as shown in Fig. 8. For $\lambda \neq 0$, the largest line-to-line voltage within a loop is

$$V_{\mathrm{dc}}^{\mathrm{rat}} = \max_{0 \leq N \leq n-1} \left\{ E_\phi \left| \sum_{\nu=0}^{N} \mathrm{e}^{\mathrm{j}\lambda\nu(2\pi/n)} \right| \right\} \tag{15}$$

where max represents the maximum obtained in its argument when $N$ varies between 0 and $n-1$, for given $n$ and $\lambda$.

From Fig. 8, the analysis corroborates the remarks from [9] concerning that, for $n = 5$, $\lambda = 1$ and $\lambda = 2$ permit lower $V_{\mathrm{dc}}$ than $\lambda = 0$. This figure also shows that, for any $n$, the minimum $V_{\mathrm{dc}}$ is very close to $2E_\phi$ for $\lambda = 0$, and to $E_\phi$ for the highest (for given $n$) $\lambda$. In addition, for each $\lambda$ (except $\lambda = 0$), the dc-link exploitation worsens with increasing $n$. In fact, for $n > 9$ the $\lambda = 1$ SWC requires $V_{\mathrm{dc}}$ to be larger in >50% compared with $\lambda = 0$. Therefore, given such gain in voltage rating, the advantage provided by $\lambda = 1$ regarding MAT and SCL might not be enough to make this SWC a suitable option when $n > 9$. Nevertheless, for $\lambda = 1$ with $n$ between six and nine, which yields substantial MAT and SCL enhancement compared with a star (see Sections 4 and 5), the voltage overrating is <50% (see Fig. 8). Furthermore, when $n > 10$, $\lambda = 2$ attains MAT and SCL close to those of $\lambda = 1$ (see Sections 4 and 5), with $V_{\mathrm{dc}}$ overrating of <25% with respect to $\lambda = 0$ (see Fig. 8).

### 6.2 Comparison of converter current rating

Fig. 9 shows the converter current rating (i.e. maximum line current) required by each $n$ and $\lambda$, for healthy (dashed) and fault (solid) conditions. The values are expressed as a percentage of $i^{\mathrm{rc}}$. The final current rating of the actual converter for certain $n$ and $\lambda$ should be the larger value between healthy and faulty drive. For a healthy situation and $\lambda \neq 0$, the amplitude of the maximum line current for given $n$ and $\lambda$ is

$$i^{\mathrm{rat}} = i^{\mathrm{rc}} \left| 1 - \mathrm{e}^{\mathrm{j}\lambda(2\pi/n)} \right|. \tag{16}$$

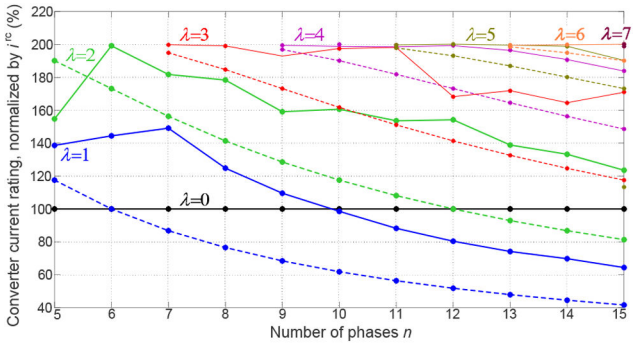


**Fig. 9** *Required converter current rating, as a function of n and the SWC, for healthy (dashed) and fault (solid) conditions*

For $\lambda = 0$ and healthy drive, $i^{\mathrm{rat}} = i^{\mathrm{rc}}$, instead. For an open leg, the current rating is obtained by numerically evaluating the line currents for torque references up to the MAT, for each $n$ and $\lambda$, and then storing the maximum line-current value (which was found to correspond to the MAT).

In agreement with [9], Fig. 9 shows that for $n = 5$ the SWCs other than star imply higher converter current rating than $\lambda = 0$. It can also be observed in this figure that in general, the current rating for given $\lambda$ tends to decrease with increasing $n$ (with a few exceptions), that for given $n$ it rises with $\lambda$ (ignoring $\lambda = 0$), and that for a faulty drive it is equal or greater than for healthy one (except for $\lambda = 2$ with $n = 5$).

Let us focus on the combination of $\lambda = 1$ with $n$ between six and nine, which was shown in the preceding study to be a good choice in terms of MAT, SCL and $V_{\mathrm{dc}}$. From Fig. 9, in such cases, the required converter current rating is greater than for star, but not by >50% (nearly, for $n = 7$).

Another advisable option, from the previous analysis, is $\lambda = 2$ with $n > 10$. According to Fig. 9, this alternative can also be considered reasonable in regard to current rating, since for these parameters, the current overrating compared with star is at most 54.2% (for $n = 12$).

Nonetheless, it cannot be concluded categorically that a certain SWC is the best (for given $n$) for any application. The purpose of this work is to contribute a comprehensive analysis that can be taken into account during the design process for choosing an option suitable for the particular requirements of each application. For instance, when postfault performance is a priority, it can be deemed worthwhile to increase the DF by using $\lambda \neq 0$ at the cost of a larger converter rating. Moreover, to ensure a specific postfault MAT for a certain drive, sometimes it can be more feasible to obtain semiconductor devices with a greater current rating (as for $\lambda \neq 0$) than a machine with higher rated current (for $\lambda = 0$).

## 7 Experimental results

### 7.1 Experimental results for six-phase induction machine

*7.1.1 Experimental setup:* The following experimental tests are carried out with a six-phase induction motor with SWA, coupled to an eddy-current brake, as shown in Fig. 10*a*. The motor is driven by two three-phase inverters (see Fig. 10*b*) based on insulated-gate bipolar transistors. The dc-link voltage $V_{\mathrm{dc}}$ is kept at 420 V by a PWM rectifier connected to the grid through a three-phase transformer and an LCL filter. The drive control is implemented in a dSPACE-MABXII-DS1401 platform. To ensure that in the steady-state, the fundamental current in each subspace equals its reference, resonant control tuned at the fundamental frequency is included in every subspace [7]. Hence, since the actual current tracks the references, the dependence of the steady-state performance (MAT, SCL and converter rating) on the control strategy can be disregarded. After a fault, the transformation (2) is not modified, but the current references in the no-torque subspaces are no longer zero [according to (7)], and one of the degrees of freedom of the control actuation is removed [5]. The $\alpha_1 - \beta_1$ current

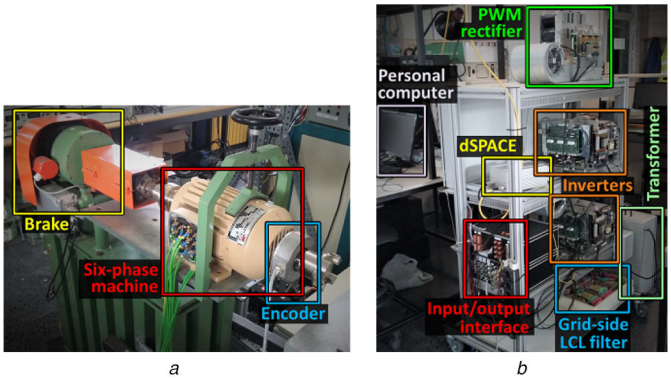


*a* *b*

**Fig. 10** *Experimental setup for n = 6*
***(a)*** Motor test bench, ***(b)*** Rest of the setup

references are set (either in healthy or fault operation) according to the widely used indirect field-oriented control [1, 3, 5, 6, 17, 28]. Accordingly, the rotor-flux position is estimated based on two variables: $i_q$ and the rotor position [28], which is measured by an encoder (see Fig. 10*a*). In the different scenarios, $i_d$ is maintained and only $i_q$ changes [5], as long as the machine operates in the base-speed region. An outer controller varies the $i_q$ reference to track the speed reference [28], which is set to 1500 r/min, while the load (and hence the torque and slip) is adjusted by the brake. The control is executed with a sampling frequency of 10 kHz, which matches the switching frequency. The deadtime is 4 $\mu$s. To facilitate the waveform inspection, switching harmonics are removed by oversampling and averaging, as in [20, 21]. Optimum zero-sequence voltages are added in the carrier-based PWM to fully exploit the dc link [21].

The current control is performed on the stator currents [transformed by (1)] rather than on the converter currents so that it is not necessary to change the machine model and so that the coefficients generated according to Section 3 can be implemented without modifications. To make this possible, the measured line currents are transformed into equivalent stator phase currents before being input to (1) and the control, and the phase-voltage references at the control output are transformed into references for the converter output voltages (with respect to the dc-link midpoint, i.e. pole voltages) before the PWM. The expressions needed to apply these transformations were priorly obtained offline by solving the systems of linear equations that relate these variables.

The six-phase motor has $N_p = 1$ pole pair, stator and rotor resistance of 6.9 and 6.3 Ω, respectively, stator and rotor leakage inductances of 2.8 and 16.6 mH, respectively, and magnetising inductance of $L_m = 652$ mH. The rated power of the original three-phase machine, before being rewound with $n = 6$, was 1.5 kW. It is assumed that in rated and healthy conditions (with the $n = 6$ winding) the amplitudes of the $d$-axis (rotor flux) and $q$-axis (torque) current are 1 and 2 A, respectively, which gives a total rated current magnitude of $i^{rc} = 2.24$ A, a rated rotor flux linkage of 652 mWb and a rated torque of 3.81 Nm. The current waveforms are expressed as percentages of $i^{rc}$, so that it is easier to verify the satisfaction of restriction (11).

Since the figures of merit analysed in this paper only apply to steady-state, no transient results are necessary, similarly to, e.g. [5, 9–11, 14, 15, 17, 23]. Steady-state experiments are carried out, for each SWC, at healthy and rated conditions, and under fault with $|i_{\alpha_1\beta_1}|$ set to the values corresponding to the MATs of every $\lambda$, as long as such MATs are not higher than the MAT of the SWC being tested. Accordingly, Table 1 displays the normalised $|i_{\alpha_1\beta_1}|$ quantities tested (cf. Fig. 3) and the respective average $i_q$ and output torque, with the latter, expressed both in Nm and as a percentage of the rated torque. In the second row, the $\lambda$ value for which the DF is equal to such normalised $|i_{\alpha_1\beta_1}|$ is pointed out. Note that $i_d = 1$ A is fixed and only $i_q$ is derated. Although Table 1 has been calculated for the base-speed region, it can be easily inferred that, since $i_d$ is reduced in the field-weakening region (see Section 2.2) [28], in the latter region the normalised MAT values (last row) would tend to become closer to the corresponding normalised $|i_{\alpha_1\beta_1}|$ values (first row). The relative differences between the normalised MATs would never be smaller than between the DFs.

**Table 1** Average torque and $i_q$ ($i_d = 1$ A) for each $|i_{\alpha_1\beta_1}|$ tested for $n = 6$

| $\lvert i_{\alpha_1\beta_1}\rvert$, % | 57.6 | 77.1 | 89.8 | 100 |
|---|---|---|---|---|
| $\lambda$ with such DF | 2 | 0 | 1 | — |
| $i_q$, A | 0.81 | 1.40 | 1.74 | 2.00 |
| torque, Nm | 1.55 | 2.68 | 3.32 | 3.81 |
| torque, % | 40.6 | 70.2 | 87.1 | 100 |

*7.1.2 Validation of MAT for $\lambda = 0$ SWC:* Fig. 11 shows the stator current and reference pole voltages for $\lambda = 0$. First, rated and healthy conditions ($|i_{\alpha_1\beta_1}| = 100\%$) can be seen in Fig. 11*a*. The phase-current (line-current) trajectory in the $\alpha_1 - \beta_1$ plane is roughly a circle of 100% radius. The other subspace currents are negligible. Current harmonics and imbalance, due to converter and machine non-linearities, are attenuated by the control [20, 21, 29]. The waveforms of reference pole voltages (and line currents) will be used later, in Section 7.1.6, to support the comparison of converter rating.

Fig. 11*b* shows the results for $\lambda = 0$ with line d open and torque set to the $\lambda = 2$ MAT ($|i_{\alpha_1\beta_1}| = 57.6\%$; cf. Table 1). The currents are unbalanced due to the fault. Most importantly, the current peaks are lower than 100%, because with $\lambda = 0$ SWC the torque (or $|i_{\alpha_1\beta_1}|$ reference) can still be increased to a larger MAT than with $\lambda = 2$, as expected from theory.

The results for the $\lambda = 0$ MAT ($|i_{\alpha_1\beta_1}| = 77.1\%$; cf. Table 1) under line d open are shown in Fig. 11*c*. The currents of all phases except the faulted one reach the boundary of 100%, which is in agreement with the fact that it is the MAT for the tested SWC ($\lambda = 0$).

*7.1.3 Validation of MAT for $\lambda = 1$ SWC:* Fig. 12 shows the results for $\lambda = 1$. From Fig. 12*a*, in healthy and rated conditions, the phase currents are similar to $\lambda = 0$ (cf. Fig. 11*a*).

In the following tests, line d – e (i.e. the line supplying $i_{de}$ in Fig. 1*b*) is open, i.e., $i_{de} = 0$. The results when the torque is set to the MAT corresponding to $\lambda = 2$ ($|i_{\alpha_1\beta_1}| = 57.6\%$) and to $\lambda = 0$ ($|i_{\alpha_1\beta_1}| = 77.1\%$) are shown in Figs. 12*b* and *c*, respectively. From these plots, the peaks of the phase currents are lower than 100%. This means that with the $\lambda = 1$ SWC the torque reference can be increased beyond the $\lambda = 2$ and $\lambda = 0$ MATs without exceeding $i^{rc}$.

The waveforms when the torque reference equals the $\lambda = 1$ MAT ($|i_{\alpha_1\beta_1}| = 89.8\%$; cf. Table 1) are shown in Fig. 12*d*. In this scenario, the currents of all phases except those connected to the faulted line (which are smaller) have amplitude roughly equal to 100%. This corroborates the conclusion from Section 4 that $\lambda = 1$ yields much larger MAT than $\lambda = 0$.

*7.1.4 Validation of MAT for $\lambda = 2$ SWC:* The results for $\lambda = 2$ are shown in Fig. 13. In a healthy situation with rated current ($|i_{\alpha_1\beta_1}| = 100\%$) the results (see Fig. 13*a*) are similar to those with the other SWCs (cf. Figs. 11*a* and 12*a*).

Fig. 13*b* shows the results under fault in line d–f and the $\lambda = 2$ MAT ($|i_{\alpha_1\beta_1}| = 57.6\%$). In this case, three out of the six phase currents reach the maximum of 100%, while the other ones cannot increase any further due to the three current constraint identities: one associated to the fault [see (10)] and two because of stator loops [see (12)]. Thus, as expected, the MAT for $\lambda = 2$ is much smaller than for $\lambda = 0$ and $\lambda = 1$.

*7.1.5 Comparison of SCL:* The SCL in each of the tests is displayed in Table 2. With healthy drive and rated current, the SCL is practically the same for the three SWCs. Dashes indicate unsuitable combinations of $|i_{\alpha_1\beta_1}|$ and $\lambda$, which require larger torque than the respective MAT. From this table, $\lambda = 1$ yields the smallest SCL for $|i_{\alpha_1\beta_1}| = 57.6\%$, and also for $|i_{\alpha_1\beta_1}| = 77.1\%$. This verifies the finding from Section 5 that the $\lambda = 1$ SWC is not only the most convenient in terms of MAT, but also of SCL.

In the previous results, the phase currents were obtained from line currents, which are the ones usually measured in drives. Consequently, the current that may circulate within the stator loops due to machine non-idealities has not been reflected so far. This circulating current corresponds to $i_{0^+}$ for $\lambda = 1$ and to both $i_{0^+}$ and $i_{0^-}$ for $\lambda = 2$. These components have been separately measured for each case, and the associated additional SCL is displayed in Table 3. This extra SCL is computed as $n(i_{0^+}^2 + i_{0^-}^2)R_s$, with $R_s$ being the nominal stator resistance. From Table 3, although the extra

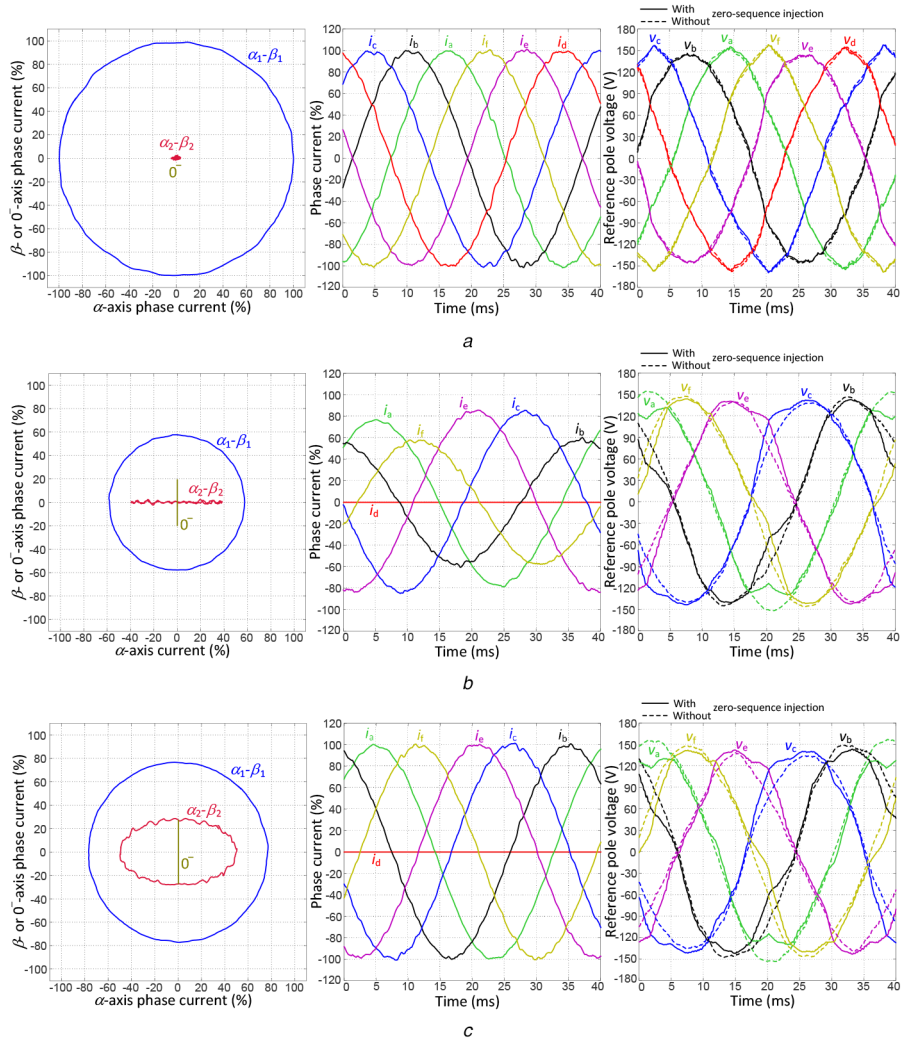


**Fig. 11** *Experimental results for $n = 6$ with the $\lambda = 0$ SWC*
***(a)*** $|i_{\alpha_1\beta_1}| = 100\%$ and healthy drive, ***(b)*** $|i_{\alpha_1\beta_1}| = 57.6\%$ and line d open, ***(c)*** $|i_{\alpha_1\beta_1}| = 77.1\%$ and line d open

SCL due to circulating current is greater for $\lambda = 2$ (which includes third-order harmonic) than for $\lambda = 1$ (mainly caused by imbalance), in both cases, it is practically negligible in comparison with the total SCL (cf. Table 2). This conclusion holds for both healthy and faulty conditions.

*7.1.6 Comparison of required converter rating:* Table 4 shows the maximum line-to-line values between the converter reference voltages (for the same winding loop or star) in steady-state for each tested case. These values were obtained from the reference pole voltages, including zero-sequence injection, as shown in Figs. 11–13. The quantities in Table 4 represent the minimum required $V_{dc}$. In accordance with Fig. 8, the necessary $V_{dc}$ is similar for $\lambda = 0$ and $\lambda = 1$, but it is roughly halved for $\lambda = 2$. The differences between the values in Fig. 8 and Table 4 are due to imbalance and harmonics caused by non-idealities, as well as to the fact that the stator-impedance voltage drop was neglected for Fig. 8. In any case, these discrepancies are relatively small, further confirming the validity of the theory. In this regard, it is also interesting to note in Figs. 11–13 that, as expected, the zero-sequence injection diminishes the effect of the voltage imbalance associated to the fault on the required $V_{dc}$ (see, e.g. Fig. 13*b*).

Table 5 displays the maximum line current in steady-state for each scenario, as a percentage of $i^{rc}/\sqrt{2}$, obtained from the line currents in Figs. 11–13. The values in Table 5 are in agreement with Fig. 9, apart from some slight deviations caused by imbalance and harmonics. Namely, from Table 5 the converter rated current should be roughly 46 and 100% larger for $\lambda = 1$ and $\lambda = 2$, respectively, than for $\lambda = 0$.

*7.1.7 Final remarks:* Therefore, as concluded from the theory, it can also be deduced from the results that $\lambda = 1$ is very convenient for $n = 6$ when postfault performance is a priority, because it permits to increase the DF from 77.1 to 89.8% (e.g. the MAT changes from 2.68 to 3.32 Nm in this setup; cf. Table 1), by raising the converter current rating in about 45% and without making $V_{dc}$ greater.

### *7.2 Experimental results for a twelve-phase permanent-magnet synchronous machine*

*7.2.1 Experimental setup:* Pictures of the power electronics and of the motor test bench of the twelve-phase experimental setup are shown in Fig. 14*a* and *b*, respectively. A three-phase induction machine is driven by a commercial variable speed drive at an approximate speed of 600 r/min. The twelve-phase permanent-magnet machine is coupled to the induction one, supplying power as a generator to the dc link of the twelve-phase PWM converter. The latter is composed of two three-phase converters and a six-phase one, all of them based on insulated-gate bipolar transistors. To maintain the dc-link voltage at 750 V, the remaining active power is applied to a resistive load by means of a controlled switching transistor. The switching frequency of the converters is 5 kHz, with a deadtime of 4 µs. The control is performed at 5 kHz in a dSPACE-MicroLabBox platform. Since the $n = 12$ machine is a salient synchronous one and it is tested in the base-speed region (see Section 2.2), the $i_d$ and $i_q$ references are set according to the (conventional) maximum-torque-per-ampere strategy [30]. The rotor position is measured by an encoder. As in the other setup,

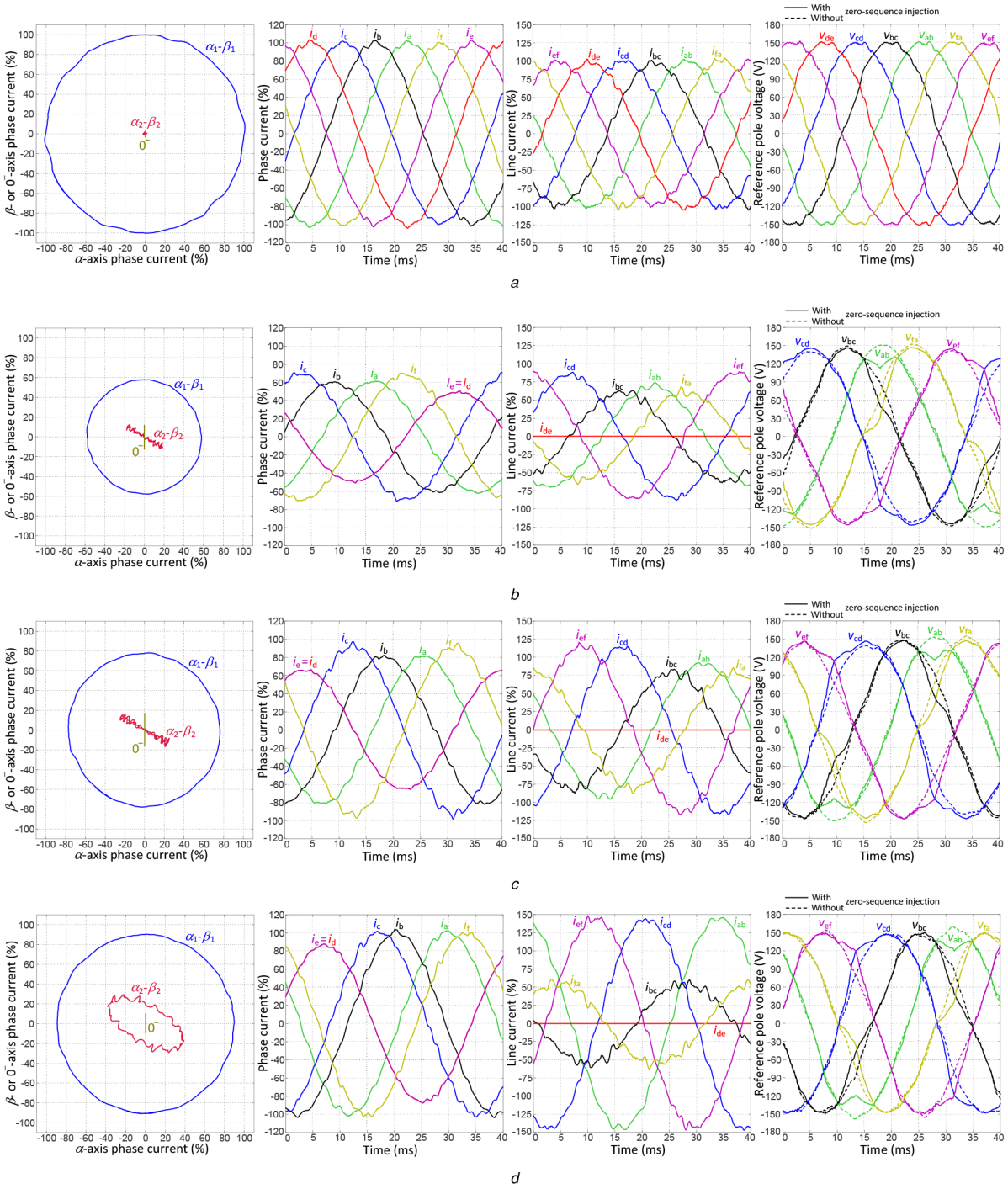


**Fig. 12** *Experimental results for $n = 6$ with the $\lambda = 1$ SWC*
***(a)*** $|i_{\alpha_1\beta_1}| = 100\%$ and healthy drive, ***(b)*** $|i_{\alpha_1\beta_1}| = 57.6\%$ and line d – e open, ***(c)*** $|i_{\alpha_1\beta_1}| = 77.1\%$ and line d – e open, ***(d)*** $|i_{\alpha_1\beta_1}| = 89.8\%$ and line d – e open

resonant control at the fundamental frequency is implemented in all subspaces [7].

The main parameters of the $n = 12$ machine are $N_p = 4$ pole pairs, rated power of 10 kW, rated phase current rms of 4 A ($i^{rc} = 5.66$ A), stator resistance of 0.7 Ω, stator leakage inductance of 0.4 mH, $d$- and $q$-axis self-inductances of $L_d = 1.6$ mH and $L_q = 2.8$ mH, and voltage constant (phase voltage in rms) of 0.1533 V/r/min.

Analogously to the $n = 6$ machine, the $n = 12$ one is also tested, for each SWC, in healthy conditions with rated current and torque, and under fault at every MAT (DFs in Fig. 3) equal or lower than the respective MAT of such SWC. The average torque, $i_d$ and $i_q$ values of each test are shown in Table 6. From this table, in this machine, the effect of saliency on the torque and optimum $i_d$ and $i_q$ is barely noticeable. In fact, the normalised MATs and the DF are nearly identical.

*7.2.2 Validation of MATs:* Although the captures are not shown here for lack of space, all the DFs assessed in Section 4 for $n = 12$ (see Table 6) have been confirmed by means of the experiments, similarly to the results discussed in Sections 7.1.2–7.1.4 for $n = 6$. The most meaningful data obtained from these $n = 12$ tests are presented in Tables 7–10 and are discussed subsequently. The fact that the values of SCL and required converter rating obtained at the MATs match the theory, as shown next, also validates indirectly that such torque values are indeed the MATs.

*7.2.3 Comparison of SCL:* Table 7 displays the SCL calculated with the stator currents of each scenario. In healthy conditions, the SCL is similar regardless of the SWC. Under open line, in agreement with the theory (see Section 5), $\lambda = 1$ provides the lowest SCL for each $|i_{\alpha_1\beta_1}|$ value, and $\lambda = 2$ achieves SCL very close to it, and substantially better than $\lambda = 0$. With the other

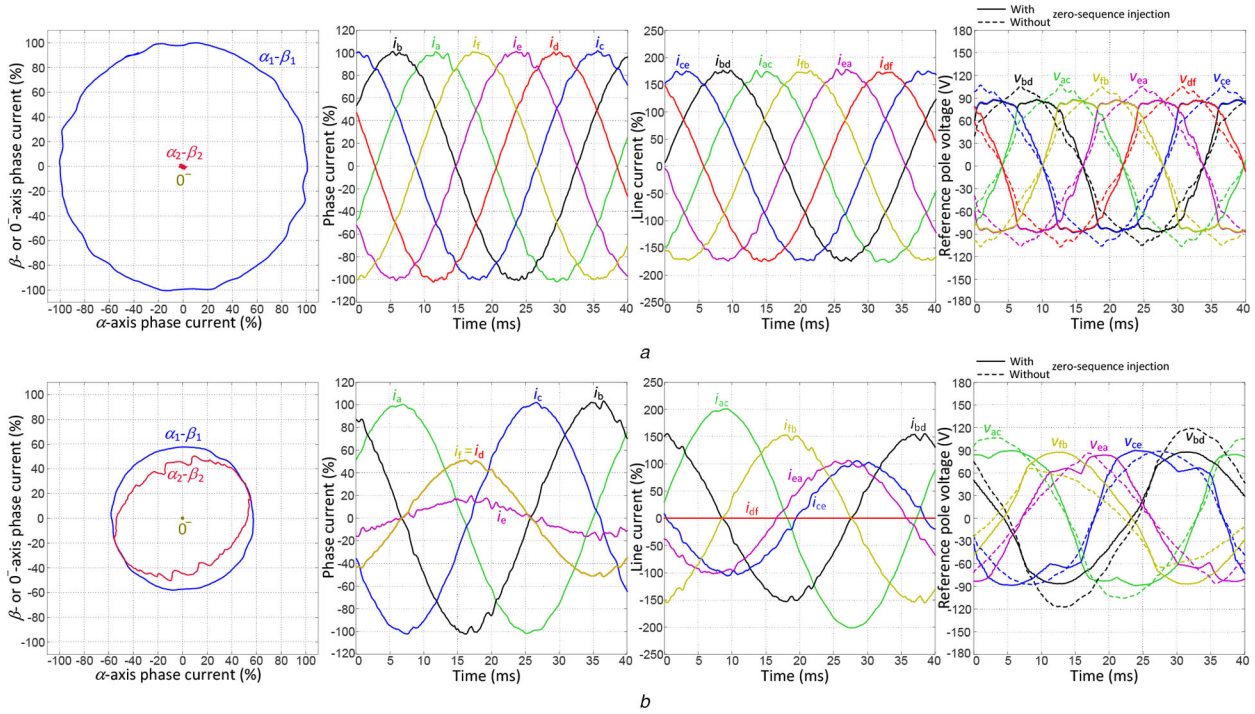


**Fig. 13** *Experimental results for $n = 6$ with the $\lambda = 2$ SWC*
***(a)*** $|i_{\alpha_1\beta_1}| = 100\%$ and healthy drive, ***(b)*** $|i_{\alpha_1\beta_1}| = 57.6\%$ and line d–f open

**Table 2** SCL in the experiments for $n = 6$

| | $\lvert i_{\alpha_1\beta_1}\rvert$, % | $\lambda = 0$, W | $\lambda = 1$, W | $\lambda = 2$, W |
|---|---|---|---|---|
| healthy | 100 | 103.0 | 103.2 | 103.8 |
| | 57.6 | 46.0 | 37.7 | 61.5 |
| open leg | 77.1 | 85.2 | 67.1 | — |
| | 89.8 | — | 94.8 | — |

**Table 3** Additional SCL in the experiments for $n = 6$ due to undesired currents circulating within the stator loops

| | $\lvert i_{\alpha_1\beta_1}\rvert$, % | $\lambda = 1$, mW | $\lambda = 2$, mW |
|---|---|---|---|
| healthy | 100 | 3 | 61 |
| | 57.6 | 2 | 46 |
| open leg | 77.1 | 3 | — |
| | 89.8 | 2 | — |

**Table 4** Maximum steady-state line-to-line converter reference voltage (within a winding loop or a star) for $n = 6$

| | $\lvert i_{\alpha_1\beta_1}\rvert$, % | $\lambda = 0$, V | $\lambda = 1$, V | $\lambda = 2$, V |
|---|---|---|---|---|
| healthy | 100 | 325.0 | 307.5 | 177.7 |
| | 57.6 | 291.0 | 297.3 | 179.5 |
| open leg | 77.1 | 291.5 | 298.3 | — |
| | 89.8 | — | 301.3 | — |

SWCs the SCL is similar or higher than $\lambda = 0$; thus, they are not recommended in this regard.

The extra SCL due to the current flowing within stator loops is reflected in Table 8. As for $n = 6$ (cf. Table 3), it is negligible in most cases. The only exception is $\lambda = 4$, where the extra SCL is much greater than in the other cases. This can be attributed to the fact that this SWC has the highest number of stator loops (four) and that in this case, a harmonic order as low as the third can give rise to circulating currents. Nonetheless, as previously mentioned, $\lambda = 4$ is not one of the recommended SWCs, but rather the opposite.

**Table 5** Maximum steady-state line current rms (% of $i^{rc}/\sqrt{2}$) for $n = 6$

| | $\lvert i_{\alpha_1\beta_1}\rvert$, % | $\lambda = 0$, % | $\lambda = 1$, % | $\lambda = 2$, % |
|---|---|---|---|---|
| healthy | 100 | 99.9 | 100.7 | 174.6 |
| | 57.6 | 84.0 | 85.2 | 200.6 |
| open leg | 77.1 | 100.1 | 114.1 | — |
| | 89.8 | — | 145.8 | — |

*7.2.4 Comparison of required converter rating:* To compare the dc-link utilisation, the maximum line-to-line values among the converter references (for the same winding loop or star) are shown in Table 9 for each scenario. In these experiments, optimum non-current-producing voltages were also injected for full dc-link exploitation [21]. Taking into account that $2E_\varphi$ at the tested speed is 260.2 V, it can be observed that the values shown in Table 9 are in agreement with the theoretical analysis in Section 6.1, particularly with Fig. 8. The small discrepancies are mainly due to the fact that the voltage drop in the stator impedance has been disregarded in theory. As shown in Fig. 8, it can be seen in Table 9 that $\lambda = 1$ requires almost twice as large $V_{dc}$ compared with $\lambda = 0$, that $\lambda = 2$ needs a similar $V_{dc}$ to $\lambda = 0$, and that the other SWCs are able to operate with lower $V_{dc}$ (at the cost of other, previously mentioned, serious drawbacks).

Finally, Table 10 shows the maximum line current rms (as a percentage of $i^{rc}/\sqrt{2}$) in steady-state, for each of the tested scenarios. These results also match with a good degree of accuracy with the theoretical ones (compare Table 10 and Fig. 9). As in Fig. 9, it can be observed in Table 10 that $\lambda = 1$ permits lower line current than $\lambda = 0$, that $\lambda = 2$ implies a similar line current rms in healthy conditions to $\lambda = 0$ and a current overrating up to ~52% under fault, and also that the other SWCs require substantially greater line current than $\lambda = 0$ for both healthy and faulty drive.

*7.2.5 Final remarks:* In summary, the results shown here for $n = 12$ further verify the theoretical analysis, and they particularly corroborate the conclusion that for relatively high phase numbers ($n > 10$, such as $n = 12$) the $\lambda = 2$ SWC is a very good option, since it avoids the large $V_{dc}$ required by $\lambda = 1$, while providing almost as good DF and SCL as $\lambda = 1$ (superior to all the other

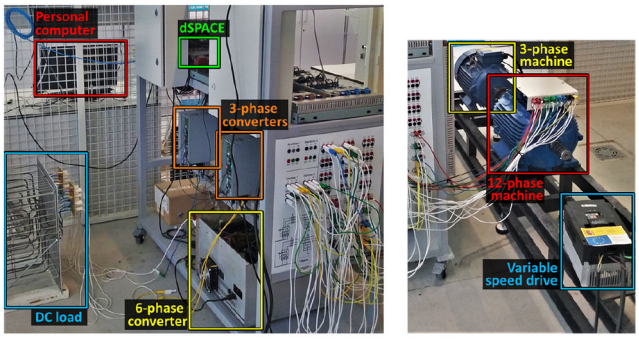


*a* *b*

**Fig. 14** *Experimental setup for $n = 12$*
***(a)*** Power electronics, ***(b)*** Test bench

**Table 6** Average torque, $i_d$ and $i_q$ for each $|i_{\alpha_1\beta_1}|$ tested for $n = 12$

| $\lvert i_{\alpha_1\beta_1}\rvert$, % | 78.8 | 82.2 | 89.9 | 90.2 | 96.8 | 99.4 | 100 |
|---|---|---|---|---|---|---|---|
| $\lambda$ with such DF | 4 | 5 | 3 | 0 | 2 | 1 | — |
| $-i_d$, A | 0.11 | 0.12 | 0.14 | 0.14 | 0.17 | 0.17 | 0.18 |
| $i_q$, A | 4.46 | 4.65 | 5.08 | 5.10 | 5.47 | 5.62 | 5.65 |
| torque, Nm | 23.2 | 24.2 | 26.5 | 26.6 | 28.5 | 29.3 | 29.4 |
| torque, % | 78.8 | 82.2 | 89.9 | 90.2 | 96.8 | 99.4 | 100 |

**Table 7** SCL in the experiments for $n = 12$

| | $\lvert i_{\alpha_1\beta_1}\rvert$, % | $\lambda = 0$, W | $\lambda = 1$, W | $\lambda = 2$, W | $\lambda = 3$, W | $\lambda = 4$, W | $\lambda = 5$, W |
|---|---|---|---|---|---|---|---|
| healthy | 100 | 134.3 | 134.7 | 134.4 | 134.7 | 134.6 | 134.9 |
| | 78.8 | 92.6 | 84.5 | 86.9 | 91.9 | 99.3 | 103.3 |
| | 82.2 | 101.0 | 91.6 | 94.8 | 101.1 | — | 117.8 |
| open leg | 89.9 | 122.0 | 109.8 | 113.4 | 121.5 | — | — |
| | 90.2 | 123.1 | 111.3 | 114.3 | — | — | — |
| | 96.8 | — | 127.8 | 134.4 | — | — | — |
| | 99.4 | — | 134.4 | — | — | — | — |

**Table 8** Additional SCL in the experiments for $n = 12$ due to undesired currents circulating within the stator loops

| | $\lvert i_{\alpha_1\beta_1}\rvert$, % | $\lambda = 1$, W | $\lambda = 2$, W | $\lambda = 3$, W | $\lambda = 4$, W | $\lambda = 5$, W |
|---|---|---|---|---|---|---|
| healthy | 100 | 0.11 | 0.11 | 0.50 | 8.04 | 0.11 |
| | 78.8 | 0.08 | 0.13 | 0.35 | 5.03 | 0.04 |
| | 82.2 | 0.08 | 0.12 | 0.38 | — | 0.05 |
| | 89.9 | 0.09 | 0.13 | 0.45 | — | — |
| open leg | 90.2 | 0.09 | 0.13 | — | — | — |
| | 96.8 | 0.09 | 0.16 | — | — | — |
| | 99.4 | 0.10 | — | — | — | — |

**Table 9** Maximum steady-state line-to-line converter reference voltage (within a winding loop or star) for $n = 12$

| | $\lvert i_{\alpha_1\beta_1}\rvert$, % | $\lambda = 0$, V | $\lambda = 1$, V | $\lambda = 2$, V | $\lambda = 3$, V | $\lambda = 4$, V | $\lambda = 5$, V |
|---|---|---|---|---|---|---|---|
| healthy | 100 | 272.8 | 530.1 | 248.8 | 172.7 | 152.4 | 127.0 |
| | 78.8 | 271.4 | 539.2 | 255.7 | 167.6 | 143.8 | 123.9 |
| | 82.2 | 272.6 | 538.8 | 254.8 | 169.8 | — | 133.5 |
| open leg | 89.9 | 273.9 | 539.1 | 253.3 | 167.6 | — | — |
| | 90.2 | 277.0 | 539.7 | 253.4 | — | — | — |
| | 96.8 | — | 538.0 | 245.7 | — | — | — |
| | 99.4 | — | 540.7 | — | — | — | — |

SWCs), and with a moderate (below 55%) current overrating for fault conditions.

Since the results confirm the validity of the theory for $n = 6$ and $n = 12$, and such a theoretical approach is essentially the same as for other $n$ values, the theoretical outcomes for other $n$ are also indirectly validated to a great extent. Similarly, these results with two setups also verify that, as expected, the analysis and its conclusions hold for different machine types, parameters, powers and switching frequencies.

## 8 Conclusion

In this paper, the performance of various SWCs is compared, under healthy situation and open converter leg, in terms of MAT (or

**Table 10** Maximum steady-state line current rms (% of $i^{rc}/\sqrt{2}$) for $n = 12$

| | $\lvert i_{\alpha_1\beta_1}\rvert$, % | $\lambda = 0$, % | $\lambda = 1$, % | $\lambda = 2$, % | $\lambda = 3$, % | $\lambda = 4$, % | $\lambda = 5$, % |
|---|---|---|---|---|---|---|---|
| healthy | 100 | 103.1 | 52.4 | 100.9 | 143.3 | 175.3 | 195.6 |
| | 78.8 | 100.6 | 60.5 | 111.0 | 135.1 | 189.7 | 197.0 |
| | 82.2 | 100.5 | 62.8 | 115.6 | 140.1 | — | 199.8 |
| open leg | 89.9 | 100.7 | 68.9 | 126.1 | 163.8 | — | — |
| | 90.2 | 100.7 | 69.5 | 127.0 | — | — | — |
| | 96.8 | — | 74.8 | 154.9 | — | — | — |
| | 99.4 | — | 81.6 | — | — | — | — |

equivalently, DF), SCL and converter rating. In contrast to SWC comparisons in previous publications, where no phase numbers $n$ greater than five were considered, here $n$ values up to fifteen are taken into account.

In healthy drive, normally the MAT and SCL barely change for different SWCs such as $\lambda = 0$ (star), $\lambda = 1$ and $\lambda = 2$, as long as the circulating current is negligible. Concerning postfault operation, it has been shown that the $\lambda = 1$ SWC provides the largest MAT and smallest SCL of all SWCs, for any $n$. Moreover, the degree of improvement (especially in MAT) becomes drastically more noticeable for $n$ higher than five, which was the only case, other than $n = 3$, studied in the existing literature. For example, by replacing $\lambda = 0$ by $\lambda = 1$, the DF increases in just 3.7% (up to 76.1%) for five phases, but in as much as 12.7% (up to 89.8%) for six phases, which was so far unknown. Actually, the DF for $\lambda = 1$ is practically 100% for most $n$ under study. Nonetheless, for $n > 9$ the converter voltage rating would have to be increased in >50% if $\lambda = 1$ were to be adopted instead of $\lambda = 0$. On the other hand, the $\lambda = 2$ SWC attains MAT and SCL close to those of $\lambda = 1$ (much larger than for $\lambda = 0$) when roughly $n > 10$, without having to raise either the converter voltage or current rating in >55% (compared with $\lambda = 0$). Thus, broadly speaking the most convenient alternatives in terms of converter rating and postfault MAT and SCL are $\lambda = 1$ with $n$ between six and nine, and $\lambda = 2$ with $n > 10$. Although these options imply increasing moderately (in <55%) the converter voltage rating (for either healthy or fault operation) or current rating (especially for fault conditions) with respect to star SWC, this can be an acceptable drawback, e.g. in applications where postfault performance is a primary concern.

It should also be highlighted that these differences with respect to $n = 5$ could not be easily inferred without carrying out the extensive analysis presented in this paper for $n > 5$.

In practice, circulating currents caused by machine non-idealities slightly increase SCL with respect to the ideal values, for SWCs different from star, with either healthy or faulty drive. This potential problem should be taken into account in the design of the winding distribution to minimise the corresponding space harmonics and imbalance. Nevertheless, since the orders of these harmonics are often even or relatively high (e.g. of sixth-order and its multiples for $n = 6$ with $\lambda = 1$ and for $n = 12$ with $\lambda = 2$), this aspect is not as critical as for the third-order current for $n = 3$ with delta SWC or even the fifth-order current for $n = 5$ with pentagon SWC. Furthermore, given the significant improvement attained by $\lambda = 1$ and $\lambda = 2$ SWCs in the scenarios pointed out, this extra SCL is usually negligible compared with it.

Experimental results with a six-phase induction machine and a twelve-phase permanent-magnet one, under healthy and faulty operation, have been presented for verification.

Some possible subjects of future research are the performance of various SWCs under several simultaneous open legs, under other types of faults, with very low sampling/switching frequencies (e.g. some multi-megawatt drives), with significant space harmonics (airgap flux harmonics, and hence overall efficiency, may change with the SWC [10]), and for machines with AWA.

## 9 References


[1] Levi, E.: 'Multiphase electric machines for variable-speed applications', *IEEE Trans. Ind. Electron.*, 2008, **55**, (5), pp. 1893–1909

[2] Levi, E.: 'Advances in converter control and innovative exploitation of additional degrees of freedom for multiphase machines', *IEEE Trans. Ind. Electron.*, 2016, **63**, (1), pp. 433–448

[3] Barrero, F., Duran, M.J.: 'Recent advances in the design, modeling and control of multiphase machines – part 1', *IEEE Trans. Ind. Electron.*, 2016, **63**, (1), pp. 449–458

[4] Duran, M.J., Barrero, F.: 'Recent advances in the design, modeling and control of multiphase machines – part 2', *IEEE Trans. Ind. Electron.*, 2016, **63**, (1), pp. 459–468

[5] Che, H.S., Duran, M.J., Levi, E., *et al.*: 'Postfault operation of an asymmetrical six-phase induction machine with single and two isolated neutral points', *IEEE Trans. Power Electron.*, 2014, **29**, (10), pp. 5406–5416

[6] Munim, W.N.W.A., Duran, M.J., Che, H.S., *et al.*: 'A unified analysis of the fault tolerance capability in six-phase induction motor drives', *IEEE Trans. Power Electron.*, 2017, **32**, (10), pp. 7824–7836

[7] Tani, A., Mengoni, M., Zarri, L., *et al.*: 'Control of multiphase induction motors with an odd number of phases under open-circuit phase faults', *IEEE Trans. Power Electron.*, 2012, **27**, (2), pp. 565–577

[8] Mohammadpour, A., Parsa, L.: 'A unified fault-tolerant current control approach for five-phase PM motors with trapezoidal back EMF under different stator winding connections', *IEEE Trans. Power Electron.*, 2013, **28**, (7), pp. 3517–3527

[9] Abdel-Khalik, A.S., Morsy, A.S., Ahmed, S., *et al.*: 'Effect of stator winding connection on performance of five-phase induction machines', *IEEE Trans. Ind. Electron.*, 2014, **61**, (1), pp. 3–19

[10] Abdel-Khalik, A.S., Ahmed, S., Elserougi, A.A., *et al.*: 'Effect of stator winding connection of five-phase induction machines on torque ripples under open line condition', *IEEE/ASME Trans. Mechatron.*, 2015, **20**, (2), pp. 580–593

[11] Abdel-Khalik, A.S., Ahmed, S., Massoud, A.M.: 'Steady-state equivalent circuit of five-phase induction machines with different stator connections under open-line conditions', *IEEE Trans. Ind. Electron.*, 2016, **63**, (8), pp. 4651–4662

[12] Mohammadpour, A., Sadeghi, S., Parsa, L.: 'A generalized fault-tolerant control strategy for five-phase PM motor drives considering star, pentagon, and pentacle connections of stator windings', *IEEE Trans. Ind. Electron.*, 2014, **61**, (1), pp. 63–75

[13] Cao, W., Mecrow, B.C., Atkinson, G.J., *et al.*: 'Overview of electric motor technologies used for more electric aircraft (MEA)', *IEEE Trans. Ind. Electron.*, 2012, **59**, (9), pp. 3523–3531

[14] Baneira, F., Doval-Gandoy, J., Yepes, A.G., *et al.*: 'Control strategy for multiphase drives with minimum losses in the full torque operation range under single open-phase fault', *IEEE Trans. Power Electron.*, 2017, **32**, (8), pp. 6275–6285

[15] Ryu, H.M., Kim, J.W., Sul, S.K.: 'Synchronous-frame current control of multiphase synchronous motor under asymmetric fault condition due to open phases', *IEEE Trans. Ind. Appl.*, 2006, **42**, (4), pp. 1062–1070

[16] Priestley, M., Farshadnia, M., Fletcher, J.: 'FOC transformation for single open-phase faults in the five-phase open-end winding topology', *IEEE Trans. Ind. Electron.*, 2020, **67**, (2), pp. 842–851

[17] Abdel-Khalik, A.S., Massoud, A.M., Ahmed, S.: 'Effect of DC-link voltage limitation on postfault steady-state performance of asymmetrical six-phase induction machines', *IEEE Trans. Ind. Electron.*, 2018, **65**, (9), pp. 6890–6900

[18] Zhang, W., Xu, D., Enjeti, P.N., *et al.*: 'Survey on fault-tolerant techniques for power electronic converters', *IEEE Trans. Power Electron.*, 2014, **29**, (12), pp. 6319–6331

[19] Lyra, R.O.C., Lipo, T.A.: 'Torque density improvement in a six-phase induction motor with third harmonic current injection', *IEEE Trans. Ind. Appl.*, 2002, **38**, (5), pp. 1351–1360

[20] Yepes, A.G., Doval-Gandoy, J., Baneira, F., *et al.*: 'Current harmonic compensation for *n*-phase machines with asymmetrical winding arrangement and different neutral configurations', *IEEE Trans. Ind. Appl.*, 2017, **53**, (6), pp. 5426–5439

[21] Yepes, A.G., Doval-Gandoy, J., Toliyat, H.: 'Multifrequency current control for *n*-phase machines including antiwindup and distortion-free saturation with full DC-bus utilization', *IEEE Trans. Power Electron.*, 2019, **34**, (10), pp. 9891–9904

[22] Hu, Y., Zhu, Z.Q., Odavic, M.: 'Torque capability enhancement of dual three-phase PMSM drive with fifth and seventh current harmonics injection', *IEEE Trans. Ind. Appl.*, 2017, **53**, (5), pp. 4526–4535

[23] Che, H.S., Hew, W.P.: 'Dual three-phase operation of single neutral symmetrical six-phase machine for improved performance'. IECON 2015 – 41st Annual Conf. of the IEEE Industrial Electronics Society, Yokohama, Japan, 2015, pp. 1176–1181

[24] Dujic, D., Jones, M., Levi, E.: 'Analysis of output current-ripple RMS in multiphase drives using polygon approach', *IEEE Trans. Power Electron.*, 2010, **25**, (7), pp. 1838–1849
[25] Yepes, A.G., Doval-Gandoy, J., Baneira, F.*, et al.*: 'Performance comparison of stator winding connections in multiphase drives under open converter leg'. 2018 IEEE Energy Conversion Congress and Exposition (ECCE), Portland, OR, USA, 2018, pp. 1776–1782
[26] Welchko, B.A., Lipo, T.A., Jahns, T.M.*, et al.*: 'Fault tolerant three-phase ac motor drive topologies: a comparison of features, cost, and limitations', *IEEE Trans. Power Electron.*, 2004, **19**, (4), pp. 1108–1116
[27] Abdel-Khalik, A.S., Masoud, M.I., Ahmed, S.*, et al.*: 'Effect of current harmonic injection on constant rotor volume multiphase induction machine stators: a comparative study', *IEEE Trans. Ind. Appl.*, 2012, **48**, (6), pp. 2002–2013
[28] Levi, E.: 'FOC: field oriented control', in Wilamowski, B.M., Irwin, J.D. (Eds.): '*The industrial electronics handbook. Vol. Power electronics and motor drives*' (CRC Press, USA, 2011, 2nd edn.)
[29] Che, H.S., Levi, E., Jones, M.*, et al.*: 'Current control methods for an asymmetrical six-phase induction motor drive', *IEEE Trans. Power Electron.*, 2014, **29**, (1), pp. 407–417
[30] Kim, S., Yoon, Y.D., Sul, S.K.*, et al.*: 'Maximum torque per ampere (MTPA) control of an IPM machine based on signal injection considering inductance saturation', *IEEE Trans. Power Electron.*, 2013, **28**, (1), pp. 488–497